

# The gravity-brightening effect and stellar atmospheres

## II Results for illuminated models with $3\,700\text{ K} < T_{\text{eff}} < 7\,000\text{ K}$

S.H.P. Alencar<sup>1</sup>, L.P.R. Vaz<sup>1</sup>, and Å. Nordlund<sup>2</sup>

<sup>1</sup> Departamento de Física, ICEX–UFMG, C.P. 702, 30.123-970 Belo Horizonte, MG – Brazil (silvia, lpv@fisica.ufmg.br)

<sup>2</sup> Niels Bohr Institute for Astronomy, Physics and Geophysics; Astronomical Observatory, Juliane Maries Vej 30, DK-2100 Copenhagen, Denmark (aake@astro.ku.dk)

Received 23 September 1998 / Accepted 18 February 1999

**Abstract.** The influence of the so-called “reflection effect” (mutual illumination in a close binary) on the gravity-brightening exponent ( $\beta$ ) is studied using the UMA (Uppsala Model Atmosphere) code. The model is applied to convective grey (in the sense of continuum-only-opacity) and non-grey (line-blanketed) atmospheres with  $3\,700\text{ K} < T_{\text{eff}} < 7\,000\text{ K}$ , illuminated by grey and non-grey fluxes. The results for grey atmospheres illuminated by grey or non-grey fluxes are very similar. In this case  $\beta$  mostly depends on the amount of incident energy and on the illumination direction, apart from the dependence on the effective temperature already discussed for non-illuminated models in a previous work (Alencar & Vaz 1997). The existence of a maximum in the  $\beta(T_{\text{eff}})$  relation is due to the interplay between the convection and opacity properties of the models. The external illumination increases the values of  $\beta$ , that is, the larger the amount of incident flux the larger the value of the exponent. This effect is caused by the “quenched” convection as the external illumination heats the surface layers of the illuminated star, thus bringing it closer to radiative equilibrium, where  $\beta$  is close to unity. We provide a polynomial fit to the variation of  $\beta$  with the fundamental parameters, in order to make it possible to easily account for the effect in light curve synthesis programs.

For line-blanketed illuminated atmospheres there is an additional dependence on the effective temperature of the incident flux (the heating temperature). This is related to the overall wavelength dependence of the spectral line opacity. Particularly in the UV, the line opacity is so strong that it prevents a significant amount of the incident flux from penetrating to the continuum formation layers. The quenching of convection by the external illumination and the related increase of  $\beta$  are thus partly prevented.

**Key words:** stars: atmospheres – stars: binaries: close – stars: binaries: eclipsing – stars: fundamental parameters – stars: general

### 1. Introduction

In order to improve the results obtained by eclipsing binary light curve models, and to avoid the multiplicity of solutions, it is convenient to keep as many parameters as possible fixed at their observed or theoretical values. The gravity-brightening exponent ( $\beta$ ) of convective atmosphere stars is usually assumed to be equal to the theoretical value  $\beta = 0.32$  (Lucy 1967),  $\beta$  being defined by the equation

$$\mathcal{F} \propto g^\beta, \quad (1)$$

proposed by von Zeipel (1924) for radiative atmospheres.

In Alencar & Vaz (1997, hereafter Paper I) it was shown that the gravity-brightening exponent of a non-illuminated convective atmosphere depends on the star’s effective temperature, Lucy’s result being a good approximation only as a mean value for non-illuminated atmospheres. In Paper I, where a brief review of the observational and theoretical work on the gravity-brightening effect was presented, it was also demonstrated that external illumination tends to increase the value of  $\beta$ .

External illumination is significant in many eclipsing binaries, as evidenced by the conspicuous “reflection effect” in their light curves. Nevertheless, until now, no particular attention has been paid to its influence on the  $\beta$  exponent. Our goal in the present study is to clarify the dependence of  $\beta$  on external illumination.

In Sect. 2 we describe our method and study the cases of grey and non-grey convective illuminated atmospheres, presenting the results (for the grey case) as a polynomial expression. Further, we explain why  $\beta$  has a maximum in the  $T_{\text{eff}}$  interval studied. We discuss the results in Sect. 3, and summarize our conclusions in Sect. 4.

### 2. The atmosphere model

We use the Uppsala Model Atmosphere (UMA, Gustafsson et al. 1975, Bell et al. 1976) code, in a version by Vaz & Nordlund (1985), as described in Paper I. The code is intended for cool ( $3\,500\text{ K} < T_{\text{eff}} < 8\,000\text{ K}$ ) atmospheres, and assumes hydrostatic equilibrium, a plane-parallel structure, and local thermo-

dynamic equilibrium. Convection is modeled with the mixing length recipe.

An illuminated model is defined by its effective temperature  $T_{\text{eff}}$ , its surface gravitational acceleration  $g$ , mixing length parameter  $\alpha = l/H_P$ , and chemical composition (fixed at solar abundance in this work). The external illumination is parameterized by the direction of illumination  $\mu$  (the cosine of the incidence angle with respect to the surface normal), the effective temperature of the illuminating star  $T_h$  and its apparent radius  $r_h$  (the ratio between the radius of the illuminating star and the distance from its centre to the surface of the reflecting star). The mixing length parameter was kept fixed at  $\alpha = 1.5$  for the illuminated models (in Paper I it was shown that the gravity-brightening exponent does not depend strongly on this parameter). We refer to models with and without spectral line absorption as “non-grey” and “grey”, respectively. The “grey” models include the variation of continuum opacity with frequency (as in Nordlund & Vaz 1990). We study grey (continuum-only) and non-grey (line-blanketed) illuminated atmospheres in convective equilibrium. The spectral lines are treated in the ODF (Opacity Distribution Function) approximation. The limits of the ODF tables constrain the effective temperature of stars in this study to a range corresponding to (ZAMS) stars with masses in the interval  $0.6 M_{\odot}$  to  $1.5 M_{\odot}$ .

### 2.1. The method

Starting from a reference ( $\log g = 4.5$ ) non-illuminated model we adjust  $T_{\text{eff}}$  for illuminated models with the same  $\log g$  until the adiabat at the bottom of the illuminated model becomes equal to that of the reference model. These models represent the illuminated and the non-illuminated sides of the same star, by having the same entropy at the bottom. We then use the illuminated model with  $\log g = 4.5$  as a reference and follow the procedure described in Paper I to determine  $\beta$ , by examining how the total flux of the illuminated models varies with  $g$  (Eq. 1).

Note that our method gives  $\beta$  as a function of parameters that were chosen primarily for convenience of computing stellar atmosphere models, rather than for their direct applicability to binary systems. The  $\log g$ ,  $r_h$ , and  $\mu$  parameters, for example, are interrelated through the value of the radius of the star. When applying these results to the study of a particular binary system, it is necessary to interpolate in our parameter space to the particular combination of parameter values appropriate to a given point on the stellar surface. The resulting values of the gravity-brightening exponent will vary between points on the reflecting stellar surface, a property that is shared with the limb-darkening coefficients, which are also affected by external illumination (Alencar & Vaz 1999).

We used suitable values for the  $\log g$  interval, to reproduce the range of distortions covered in Paper I. Eq. (1), proposed by von Zeipel (1924) for atmospheres in radiative equilibrium and applied by Lucy (1967) to stars with convection, proved to be a good approximation for all the intervals used. The correlation coefficients in the linear regressions used to determine  $\beta$  were always close to unity (the smallest one found was 0.987).

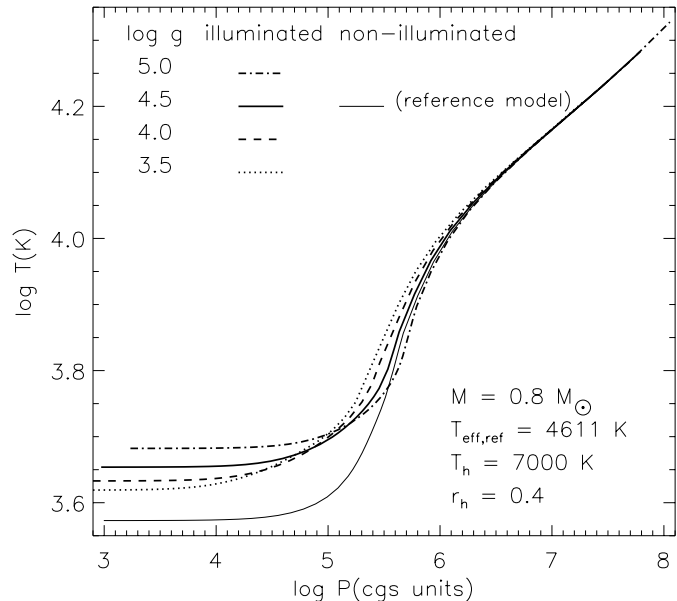


**Fig. 1.**  $\log T$  vs.  $\log P$  for convective grey non-illuminated (solid thin line) and illuminated models with  $\alpha = 1.5$ ,  $\mu = 0.93$ .

The values of  $T_{\text{eff}}$ ,  $T_h$  and of the relative flux,

$$F_{\text{rel},\mu} = [T_h/T_{\text{eff}}]^4 r_h^2 \mu, \quad (2)$$

used in the present work are representative of values for detached, semi-detached, and Algol systems found in the literature (Alencar & Vaz 1999).

In Sect. 2.2 we present the results obtained with grey atmosphere models illuminated by grey and non-grey fluxes. Initially we used  $T_h = 3700$  K,  $4500$  K,  $7000$  K and  $T_h = 10000$  K to check for a possible correlation between  $\beta$  and  $T_h$ . However, the correlation turned out to be between  $\beta$  and the relative flux and we chose to compute most of the models with  $T_h = 7000$  K. The illuminating non-grey fluxes with  $T_h \leq 7000$  K were generated with the UMA code, while for  $T_h = 10000$  K we took the fluxes from Kurucz (1979). The grey fluxes were generated from a standard grey model (see, e.g. Mihalas 1978). It is worth mentioning that, even in our most extreme case of external illumination ( $T_{\text{eff}} = 6700$  K,  $F_{\text{rel}} = 1.5$ ), the “heated” effective temperature of the illuminated models (keeping the constraint on the entropy at the bottom) did not exceed the validity limit of UMA, staying within  $T_{\text{eff}}^{\text{heated}} \lesssim 8000$  K.

In Sect. 2.3 we give the results obtained with non-grey atmospheres illuminated by grey and non-grey fluxes. In this case  $\beta$  does depend on  $T_h$ , and  $F_{\text{rel},\mu}$  alone is no longer sufficient to account for the correlations found.

### 2.2. Convective grey (continuum-only) atmospheres

Some of the models obtained with this method are shown in Fig. 1. The solid lines represent our reference models (with  $\log g = 4.5$ ); the thin line represents the non-illuminated model, while the thick line is the illuminated one. The other models are the illuminated and distorted ones. The relation of  $\log T$  to  $\log P$  is

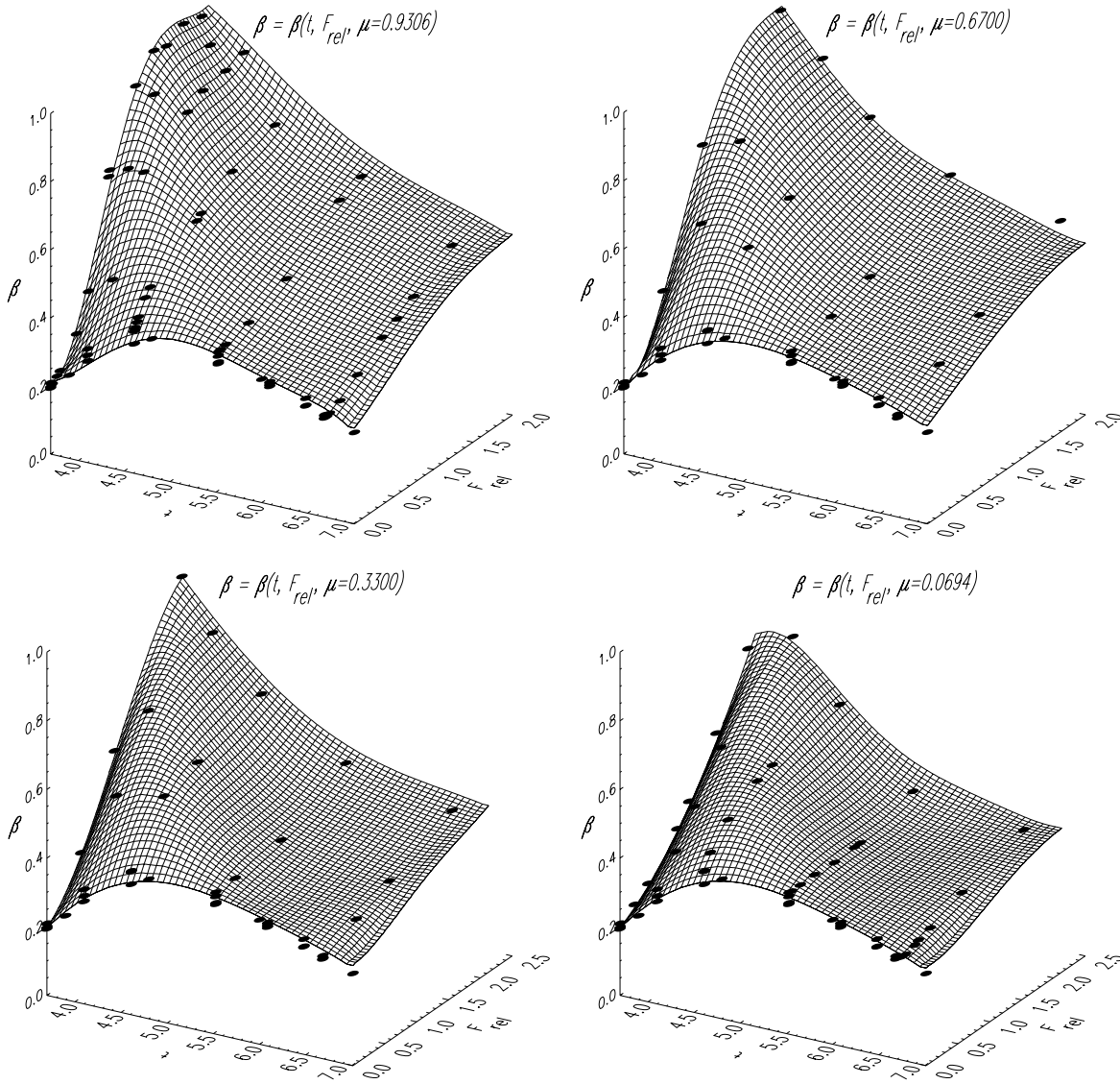


**Fig. 2.**  $\beta(t, F_{\text{rel}, \mu}, \mu)$ : calculations (grey models) and parametric surfaces (see Eq. (4) to (6)), presented for 4 values of  $\mu$ . The curved grids represent the parameterization whose coefficients are shown in Table 1, and the points represent the calculations.

the same at the bottom of the atmospheres so that the different models have the same entropy at the bottom, as discussed above.

We calculated models by varying  $r_h$  and  $T_h$  for different values of  $T_{\text{eff}}$  (illuminated atmosphere), and four values of the angle of incidence of the radiation ( $\mu = \cos \theta = 0.06943, 0.33001, 0.66999$  and  $0.93057$ ). The corresponding  $\beta$  values are shown in Fig. 2, where  $F_{\text{rel}, \mu}$  (Eq. 2), represents the influence of the parameters related to the illuminating flux, and  $t = T_{\text{eff}} \times 10^{-3}$  is the relevant parameter of the illuminated atmosphere. Note that in all panels of Fig. 2 the curve for  $F_{\text{rel}, \mu} = 0$  corresponds to the results of Paper 1 (no external illumination). Note also that  $\beta$  depends strongly on the amount of external illumination, represented by  $F_{\text{rel}, \mu}$ . A weaker dependence on the angle of incidence of the external radiation,  $\mu$ , is also visible.

The  $\beta$  exponent increases with the incident flux, represented by  $F_{\text{rel}, \mu}$  and saturates when  $\beta$  reaches its value for radiative

atmospheres. This is most noticeable for models computed with incidence direction close to the surface normal ( $\mu = 0.93$  and  $0.67$ ) in Fig. 2.

The general trend revealed in Paper 1 of  $\beta$  having a maximum for a certain value of  $T_{\text{eff}}$  is repeated here for all values of  $F_{\text{rel}, \mu}$ . The maximum shifts to lower  $T_{\text{eff}}$  with increasing values of  $F_{\text{rel}, \mu}$ .

### 2.2.1. The behaviour of $\beta$ for non-illuminated models

The maximum in  $\beta(T_{\text{eff}})$  is caused by changes in the convection and opacity properties of the models. For low  $T_{\text{eff}}$ , convection is rather efficient, because of the high mass densities and low total energy fluxes. The entropy jump at the surface is correspondingly small and its changes even smaller, yielding small  $\beta$  when we force the entropy at the bottom of the models to be

**Table 1.**  $c_{nlj}$  coefficients for Eqs. (4)-(6), corresponding to the parametric surfaces of Fig. 2 (grey models). All calculations were performed with double precision. The number inside parentheses is the power of 10 by which the entry must be multiplied (e.g.  $c_{050} = -0.00186340$ ).

$a_0$				
	$c_{010}$	$c_{011}$	$c_{012}$	$c_{013}$
$b_{00}$	1.24496 (0)	7.86878 (1)	-3.32836 (2)	3.26944 (2)
$b_{01}$	-3.37761 (0)	-7.49532 (1)	3.17539 (2)	-3.12273 (2)
$b_{02}$	1.96572 (0)	2.82025 (1)	-1.19617 (2)	1.17755 (2)
$b_{03}$	-4.55033 (-1)	-5.24475 (0)	2.22605 (1)	-2.19342 (1)
$b_{04}$	4.73747 (-2)	4.82560 (-1)	-2.04876 (0)	2.02029 (0)
$b_{05}$	-1.86340 (-3)	-1.75850 (-2)	7.46664 (-2)	-7.36785 (-2)
$a_1$				
	$c_{110}$	$c_{111}$	$c_{112}$	$c_{113}$
$b_{10}$	-2.62765 (0)	3.38727 (3)	-1.01772 (4)	6.82868 (3)
$b_{11}$	-9.75380 (0)	-3.29553 (3)	9.81068 (3)	-6.56626 (3)
$b_{12}$	8.06846 (0)	1.26666 (3)	-3.73692 (3)	2.49471 (3)
$b_{13}$	-2.24768 (0)	-2.40423 (2)	7.03300 (2)	-4.68350 (2)
$b_{14}$	2.68404 (-1)	2.25419 (1)	-6.54300 (1)	4.34712 (1)
$b_{15}$	-1.17767 (-2)	-8.35587 (-1)	2.40850 (0)	-1.59682 (0)
$a_2$				
	$c_{210}$	$c_{211}$	$c_{212}$	$c_{213}$
$b_{20}$	1.29112 (2)	-9.98733 (3)	2.78191 (4)	-1.86921 (4)
$b_{21}$	-1.12583 (2)	9.63611 (3)	-2.66734 (4)	1.79080 (4)
$b_{22}$	3.89523 (1)	-3.67200 (3)	1.01055 (4)	-6.77833 (3)
$b_{23}$	-6.70992 (0)	6.91170 (2)	-1.89208 (3)	1.26791 (3)
$b_{24}$	5.76212 (-1)	-6.42985 (1)	1.75181 (2)	-1.17284 (2)
$b_{25}$	-1.97307 (-2)	2.36651 (0)	-6.42031 (0)	4.29475 (0)
$a_3$				
	$c_{310}$	$c_{311}$	$c_{312}$	$c_{313}$
$b_{30}$	-1.95456 (2)	7.51194 (3)	-2.01052 (4)	1.34888 (4)
$b_{31}$	1.80820 (2)	-7.19551 (3)	1.91845 (4)	-1.28727 (4)
$b_{32}$	-6.62234 (1)	2.72277 (3)	-7.23386 (3)	4.85339 (3)
$b_{33}$	1.20214 (1)	-5.09115 (2)	1.34832 (3)	-9.04429 (2)
$b_{34}$	-1.08251 (0)	4.70739 (1)	-1.24314 (2)	8.33660 (1)
$b_{35}$	3.87011 (-2)	-1.72301 (0)	4.53872 (0)	-3.04289 (0)
$a_4$				
	$c_{410}$	$c_{411}$	$c_{412}$	$c_{413}$
$b_{40}$	5.85147 (1)	-1.64930 (3)	4.32086 (3)	-2.90577 (3)
$b_{41}$	-5.41777 (1)	1.57005 (3)	-4.10386 (3)	2.76141 (3)
$b_{42}$	1.98294 (1)	-5.90521 (2)	1.54029 (3)	-1.03671 (3)
$b_{43}$	-3.59233 (0)	1.09786 (2)	-2.85819 (2)	1.92392 (2)
$b_{44}$	3.22512 (-1)	-1.00971 (1)	2.62425 (1)	-1.76645 (1)
$b_{45}$	-1.14890 (-2)	3.67784 (-1)	-9.54449 (-1)	6.42438 (-1)

constant. This can be observed in Fig. 3, where we show  $\log T$  vs.  $\log P$  for a set of 5 values of  $T_{\text{eff}}$  and 4 values of  $\log g$  ( $F_{\text{rel}} = 0$ ). The effective temperature may be approximated by  $T_{\tau=2/3}$  (marked in Fig. 3). The total flux is proportional to  $\sigma T_{\text{eff}}^4$  and, using Eq. (1),  $\beta$  is thus proportional to the total extension of  $\Delta T_{\tau=2/3}$  obtained for each  $T_{\text{eff}}$  and models with  $\log g$  varying between 3.5 and 5.0 (the vertical bars in Fig. 3).

The  $T_{\text{eff}} = 3900$  K models are so adiabatic that  $\beta$  is small (the points at  $T_{\tau=2/3}$  almost follow one adiabat). For intermediate  $T_{\text{eff}}$ , convection becomes less efficient, with a correspondingly larger entropy jump near the surface. The stabilizing influence of convection thus diminishes, and the values of  $\beta$  increase (as

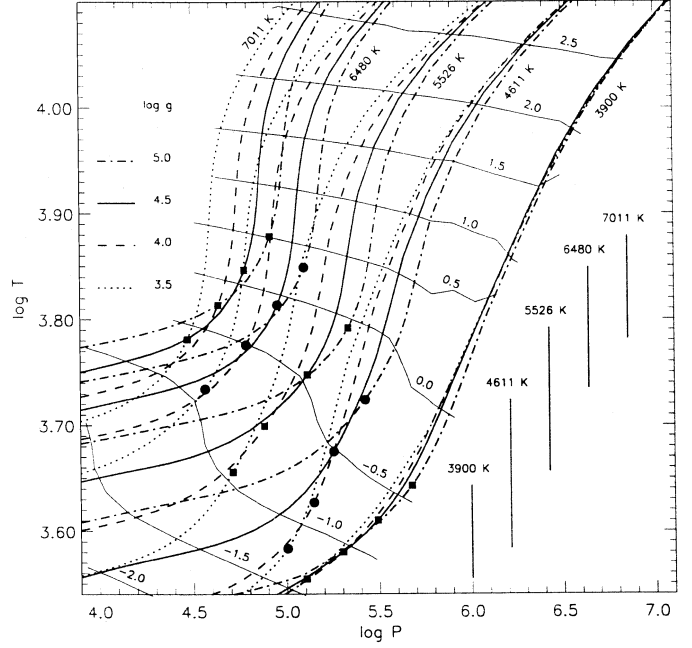


**Fig. 3.**  $\log T$  vs.  $\log P$  for convective non-grey non-illuminated models with  $\alpha = 1.5$ ,  $\mu = 0.93$  and different values of  $T_{\text{eff}}$ . For each value of  $T_{\text{eff}}$  there are 4 models with different values of  $\log g$ , which match the entropy of the reference model ( $\log g = 4.5$ ) at the bottom. The  $\blacksquare$  and  $\bullet$  symbols mark the  $\tau_{\text{Ross}} = 2/3$  (Rosselland mean) layers. The vertical bars mark the extension of the temperature variation with the different  $\log g$  for each  $T_{\text{eff}}$  at  $\tau_{\text{Ross}} = 2/3$ . The length of these bars is proportional to  $\beta$ . The thin continuous lines are contours of  $\log \kappa$  (again shown as Rosselland mean) constant, labelled from  $\log \kappa = -2.0$  to 2.5 in equal steps of 0.5 dex.

illustrated by the increase of the extension of the vertical bars in Fig. 3 for  $T_{\text{eff}} \lesssim 5500$  K).

For even higher  $T_{\text{eff}}$  the influence of the opacity becomes significant. The temperature dependence of  $\kappa$  (i.e.  $\partial \log \kappa / \partial \log T$ ) is much larger than its pressure dependence ( $\partial \log \kappa / \partial \log P$ ). This is clear from Fig. 3, which shows that the contour levels of constant  $\log \kappa$  tend to run parallel to the  $\log P$  axis, especially as  $\log T$  increases. The physical reason for this is that  $T_{\text{eff}}$  enters the regime where H is the dominant electron contributor and where, consequently, hydrogen ionization implies that the opacity (predominantly  $\text{H}^-$ ) increases very rapidly with temperature. To appreciate how the temperature sensitivity of  $\kappa$  influences  $\beta$  it is useful to consider the approximation  $\tau \sim \kappa P/g$ , according to which, if  $g$  is increased, it does not take much of an increase in  $T$  to compensate for the change. One may derive

$$\beta \approx \frac{\Delta \log T^4}{\Delta \log g} \approx \frac{4}{\left[ \frac{\partial \log \kappa}{\partial \log T} \right]_P + \left[ 1 + \left[ \frac{\partial \log \kappa}{\partial \log P} \right]_T \right] / \frac{d \log T}{d \log P}}, \quad (3)$$

where  $d \log T / d \log P$  is the logarithmic temperature gradient of the model at  $\tau = 2/3$ , and the dependence of  $d \log T / d \log P$  on  $g$  has been ignored. Eq. 3 shows that  $\beta$  does indeed become small for large values of  $\left[ \frac{\partial \log \kappa}{\partial \log T} \right]_P$ .

As discussed further below (see Sect. 3), an increasing external flux tends to extinguish convection. Illuminated models thus tend to approach radiative equilibrium, and hence  $\beta$  increases as the amount of illumination increases.

After Paper I was published, Claret (1998) submitted a work dealing with the calculation of the gravity-brightening exponent (and of limb-darkening coefficients as well) using a different approach. By using a modified version of the triangles technique (Kippenhahn et al. 1967), Claret (1998) computed  $\beta$  values of non-illuminated models for a  $T_{\text{eff}}$  interval larger than in Paper I. His results are presented as a function of the logarithm of the model masses, starting at the Solar mass. Considering values at the ZAMS, the temperature interval of  $3.56 < \log T_{\text{eff}} < 3.85$ , covered in our work, corresponds to  $-0.222 < \log(m/M_{\odot}) < 0.176$ . Claret's (1998) results are in good agreement with those from Paper I with respect to the behaviour of  $\beta$  in the common region ( $3.81 < \log T_{\text{eff}} < 3.85$ ) covered by both works.

The lower limit in  $\log T_{\text{eff}}$  of Claret's models (3.81) is larger than the value for which we found a maximum in  $\beta$  (at  $\log T_{\text{eff}} \approx 3.74$ ,  $F_{\text{rel}} = 0$ ). However, his calculation of the evolution of  $\beta$  with age for two of the models does confirm the existence of such a feature (see his Fig. 5, for the evolution of a  $2 M_{\odot}$  model off the Main Sequence, and his Fig. 6. for the evolution of a  $1 M_{\odot}$  model from the Pre-Main Sequence phase). There is no specific comment about this behaviour in his work and Claret (1998) interprets the general trends in  $\beta$  changes in terms of convection only. However, as explained above, this behaviour is due to the interplay between the convection and opacity properties of the models.

### 2.2.2. A polynomial approximation for $\beta$

The variation of  $\beta$  for illuminated grey atmospheres is primarily a function of  $T_{\text{eff}}$ ,  $F_{\text{rel},\mu}$  and  $\mu$ . In order to easily account for this dependence in light curve synthesis programs, we separate each variable using polynomials:

$$\beta = \sum_{n=0}^4 a_n(t, \mu) F_{\text{rel},\mu}^n \quad (4)$$

$$\text{where } a_n(t, \mu) = \sum_{l=0}^5 b_{nl}(\mu) t^l \quad (5)$$

$$\text{and } b_{nl}(\mu) = \sum_{m=0}^3 c_{nlm} \mu^m, \text{ with } t = T_{\text{eff}} \times 10^{-3} \quad (6)$$

The theoretical grid obtained is shown in Fig. 2, with the values determined from the atmosphere model overplotted. The 120  $c_{nlj}$  coefficients obtained with grey models are listed in Table 1. The standard deviation of the parametric fit is  $\sigma = 0.022$  (26 models), with no systematic tendency of  $\sigma$  with the incidence angle. Due to the numeric operations involved, we advise the use of the full precision given in Table 1, in order to keep errors  $\leq 0.1\%$  when calculating  $\beta$  from Eqs. (4)-(6). Care must be taken in any attempt to extrapolate beyond the limits given in Fig. 2.

In Fig. 4 we show  $\beta$  calculated for grey atmospheres ( $T_{\text{eff}} = 3697 \text{ K}$ ,  $\mu = 0.9306$ ) illuminated by grey and non-grey fluxes for different values of  $T_h$  (3 700 K, 4 500 K, 7 000 K and 10 000 K). Our parametric approximation (Eqs. 4-6) is also included. One can see that  $\beta$  does not depend significantly on  $T_h$  for grey

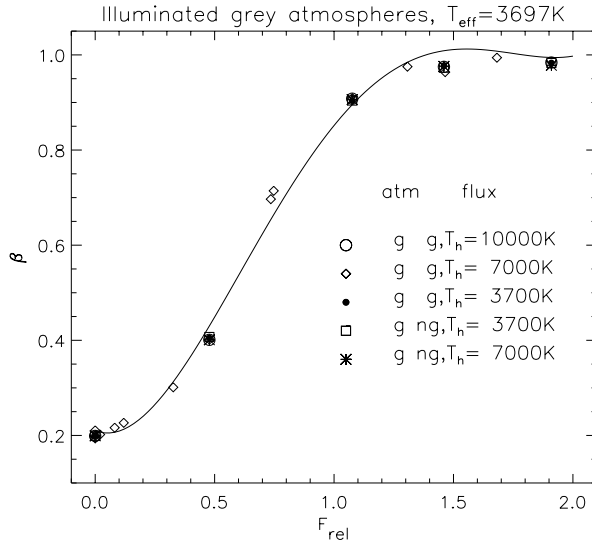


**Fig. 4.**  $\beta(F_{\text{rel},\mu=0.9306})$ , for grey atmospheres illuminated with grey (g) and non-grey (ng) fluxes with different values of  $T_h$ . The solid line corresponds to our parameterization given by Eqs. (4) to (6) and the coefficients in Table 1.

illuminated models. Similar results are obtained for grey models with other values of  $\mu$  and of  $T_{\text{eff}}$ .

### 2.3. Convective non-grey (line-blanketed) atmospheres

Using the same procedure as in Sects. 2.1 and 2.2 we constructed non-grey atmosphere models illuminated by grey and non-grey fluxes. The gravity-brightening exponent values obtained are close to the grey ones for effective temperatures of the illuminating stars ( $T_h$ ) close to those of the illuminated stars ( $T_{\text{eff}}$ ). However, for a given illuminated star and a fixed incident flux,  $\beta$  decreases with the effective temperature of the illuminating star, showing that there is a dependence of  $\beta$  on  $T_h$  beyond the dependence through the incident flux ( $\propto T_h^4$ ).

The differences between model atmospheres illuminated by grey and non-grey fluxes are small relative to the differences between the grey and non-grey illuminated models. Thus, significant changes of  $\beta$  are not related to the use of line-blanketed illuminating fluxes, but rather to the interaction between a line-blanketed illuminated atmosphere and the overall spectral distribution of the illuminating flux. Representative results are shown in Fig. 5, for a particular line-blanketed illuminated atmosphere ( $T_{\text{eff}} = 3697 \text{ K}$ ) and different illuminating fluxes (a result obtained with a grey illuminated model is shown for comparison).

It is clear from Fig. 5 that at least one more parameter is influencing the results in the case of non-grey illuminated models. By comparing the illuminated grey and non-grey models we realized that the main difference between them is that the spectral line opacity prevents part of the incident flux from reaching the continuum formation layers in the non-grey models. Because most of the spectral line opacity occurs in the UV, an increasing amount of the incident flux is intercepted for increasing effective temperatures of the illuminating star. The more of the incident

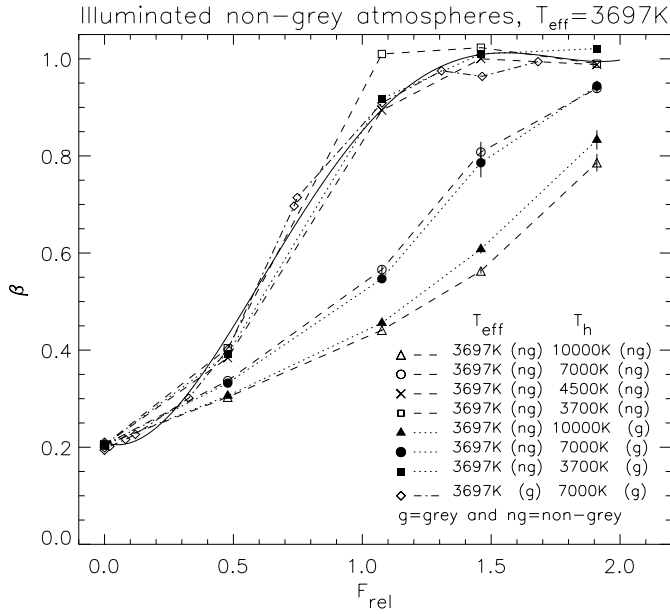


**Fig. 5.**  $\beta(t, F_{\text{rel}, \mu})$ , for non-grey atmospheres illuminated by grey (g) and non-grey (ng) fluxes with different values of  $T_h$ . The solid line has the same meaning as in Fig. 4.

flux that is intercepted, the smaller is the influence of the illumination on the convection. As a consequence, the increase of  $\beta$  with increasing illumination is reduced in non-grey models relative to grey models.

### 3. Discussion

The values of the  $\beta$  exponent in grey atmospheres illuminated by grey and non-grey fluxes are very similar. In these models  $\beta$  primarily depends on the effective temperature of the illuminated star, the relative flux and the illumination direction. The exponent increases as the relative flux increases, until it approaches the von Zeipel value ( $\beta = 1$ ) for radiative stars.

Non-grey atmospheres illuminated by grey and non-grey fluxes also have similar  $\beta$ , but for these atmospheres  $\beta$  also depends on the effective temperature of the illuminating star,  $T_h$ . In line with the discussion above, this extra dependence may be thought of in terms of how much of the incident flux reaches the continuum formation layers of the illuminated atmosphere. As  $T_h$  increases, the  $\beta$  values decrease, following nevertheless a similar behavior as a function of the relative flux, as can be seen in Fig. 5.

Some models in Fig. 5 (e.g.,  $T_{\text{eff}} = 3697$  K illuminated with  $T_h = 3700$  K and  $F_{\text{rel}} > 1$ ) have  $\beta$  values slightly larger than 1 (by  $\lesssim 3\%$ ). These values are consistent with unity within the errors of our method, and may be a numerical artifact. For grey models the  $\beta$  values return to unity for even larger values of  $F_{\text{rel}}$ , and for non-grey models a similar asymptotic behavior may be expected. It is somewhat inconsistent to consider models with large values of  $F_{\text{rel}}$  and  $T_h \sim T_{\text{eff}}$ , though, since the geometrical parameters needed would not be physically meaningful (e.g. the apparent radius would imply one star touching

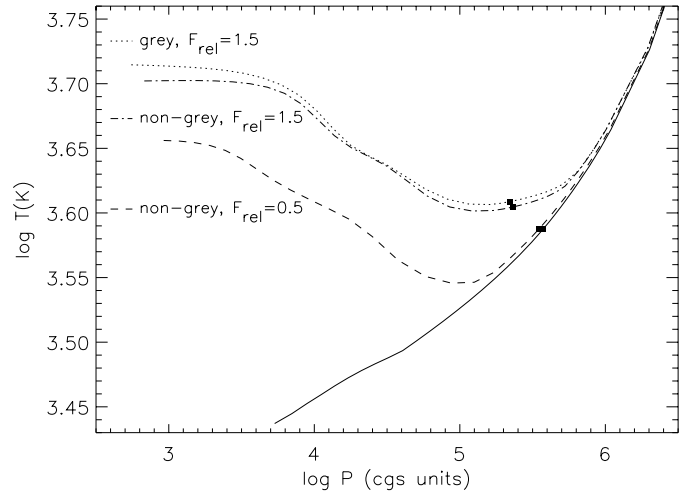


**Fig. 6.**  $\log T$  vs.  $\log P$  for convective non-grey non-illuminated (solid line) model with  $T_{\text{eff}} = 3697$  K and the same model illuminated by grey and non-grey fluxes with  $T_h = 10000$  K,  $\mu = 0.93$  and different relative fluxes. The  $\blacksquare$  signs mark the  $\tau = 2/3$  layers, as in Fig. 3.

or even intersecting the other). However, if one performs the calculation, the asymptotic behavior is indeed found also for the non-grey illuminated models, with  $\beta \lesssim 1$  for  $F_{\text{rel}} \sim 2.2$ . On the other hand, Eq. (3), in principle, does not prevent  $\beta > 1$  values. For instance, for an adiabatic ideal gas with  $\kappa$  constant and  $\frac{d \log T}{d \log P} = 2/5$ , one would have  $\beta = 8/5$ . For a real gas, if the opacity increased sufficiently slowly with temperature and pressure, and  $\frac{d \log T}{d \log P}$  was sufficiently large, Eq. (3) would allow  $\beta > 1$  values, also.

The asymptotic approach to the von Zeipel value of the gravity-brightening exponent may be understood as follows: When a model atmosphere is heated by a large external flux, a significant part of the convection is extinguished (hence most of its original flux vanishes) and the model practically becomes one in radiative equilibrium, obeying the von Zeipel law asymptotically. This is illustrated in Fig. 6 where we show a non-grey model with  $T_{\text{eff}} = 3697$  K illuminated by grey and non-grey fluxes with  $T_h = 10000$  K and two  $F_{\text{rel}, \mu}$  values. The greater the amount of external illumination, the more the model deviates from the  $\log T$  vs.  $\log P$  relation characteristic of convective equilibrium. This happens especially for  $\tau \lesssim 1$  and affects deeper layers as the amount of external illumination increases.

However, as  $T_h$  increases, the external heating flux is shifted towards the UV. Due to the larger photospheric absorption in UV, the external flux penetrates less into the photosphere of the illuminated model, and hence convection is less affected. The smaller change in convection yields a smaller  $\beta$  value, and the effect of increasing the exponent is pushed to higher relative fluxes. An immediate consequence is that line-blanketed illuminated atmospheres have  $\beta$  values which must depend on the metal abundance  $[\text{Fe}/\text{H}]$  of the model.

Somewhat more subtle effects could result from the interference of spectral line patterns in the illuminating and illuminated stars. As a particular case, when similar stars orbit each other in

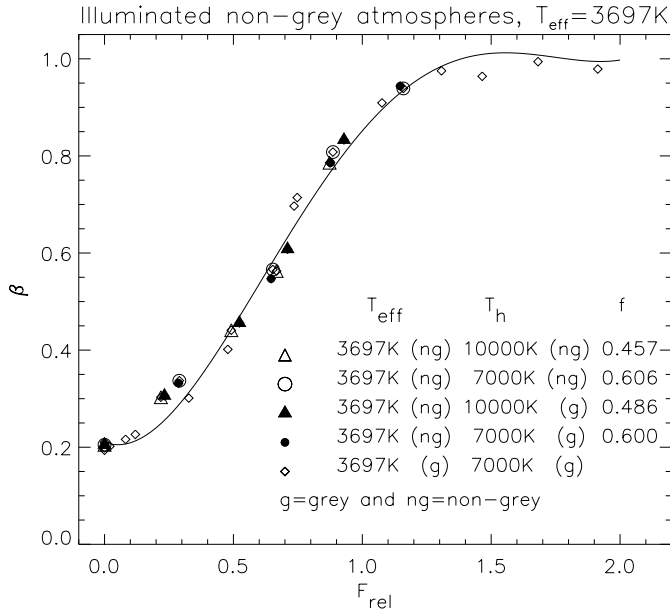


**Fig. 7.** Penetration factors ( $f$ ) for the models presented in Fig. 5. The symbols are the same as in Fig. 5, the larger symbols correspond to the corrected relative fluxes. The solid line has the same meaning as in Fig. 4.

elliptical orbits, the spectral line patterns of the stars will match optimally at apogee and perigee, and there will be a corresponding maximum in the amount of illumination of the continuum layers. For non-zero Doppler shifts the illumination of the continuum layers will decrease. However, the size of this effect is only of the order of the difference between grey and non-grey illuminating models. As mentioned above, this difference is, in general, small.

### 3.1. The penetration factor

In light of the discussion of the non-grey results of Sect. 2.3, the results for grey models obtained in Sect. 2.2 are more general than they might seem at first sight. The relative fluxes in the non-grey case should be regarded as the effective amount of flux that penetrates to the continuum formation layers. We may describe this effect through a “penetration” factor,  $f$ , that, multiplied by the incident flux, gives a new corrected flux that may be used to interpolate  $\beta$  with the grey parameterization coefficients given in Table 1 ( $F_{\text{rel},\mu} = fF_{\text{rel},\mu,\text{Total}}$ ). For grey illuminated atmospheres  $f = 1$ , while  $f < 1$  for line-blanketed illuminated models. This interpretation is strictly correct only if there exists a unique “penetration” factor for each set of parameters ( $T_{\text{eff}}$ ,  $T_{\text{h}}$  and  $\mu$ ). Fig. 7 shows the models presented in Fig. 5. It illustrates that it is indeed possible to find a factor  $f$  that brings together all the points for each set of parameters  $T_{\text{eff}}$ ,  $T_{\text{h}}$  and  $\mu$  to be fitted by the parametric curves given by Eqs. (4) to (6) and the coefficients of Table 1.

Fig. 7 shows that  $f$  differs between cases where the incident flux is a continuum-only (g) or a line-blanketed (ng) one. This is

due to minor differences in the amount of flux in the UV region. However, to a good approximation we may assume that the penetration factor is related only to the opacity distribution of the illuminated model. The surfaces presented in Fig. 2 may then be used to determine  $\beta$  even in the non-grey case, using appropriate values for the incident flux and the penetration factor.

In the present work we have concentrated on establishing the existence of such a penetration factor, by empirically calculating it and showing that it is the same for each family of models. However, it should be possible to calculate  $f$  from a knowledge of the effective temperature of the incident flux (amount of UV) and of the opacity properties of the atmosphere model in the upper layers (determining how much of the UV flux that is blocked). Studies of how to actually compute this factor for each situation are in progress and will be published elsewhere.

### 3.2. Possible tests

The secondaries of Algol-type systems are convective stars with effective temperatures around 5 000 K and may be used, with some caution, to test the gravity-brightening exponents determined here. The main problem with Algol systems is the transfer of mass between the components, which frequently causes distortion of the light curves due to spots on the stars. Nevertheless, some of these systems, whose absolute parameters are well-determined have been satisfactorily fitted with Lucy’s value 0.32 kept fixed (e.g. TV Cas, Khalessheh & Hill 1992; AT Peg, Maxted et al. 1994; HU Tau, Maxted et al. 1995). In Algol-type systems  $T_{\text{h}}$  is much greater than the secondary’s effective temperature ( $T_{\text{h}} \approx 10\,000$  K) yielding a large relative flux ( $F_{\text{rel},\mu} > 1.0$ ) and consequently a value of  $\beta$  much greater than 0.32, if we use the results obtained with grey atmospheres. But the results presented in the last section show that, in this case ( $T_{\text{h}} \gg T_{\text{eff}}$ ), the value of the exponent decreases substantially from the value obtained with grey illuminated atmospheres. This is a reassuring point for our predicted  $\beta$  values, since, even taking into account the difficulties in modeling Algols, it is expected from the published results that  $\beta$  should not differ very much from Lucy’s value. In most of the cases the authors had to let the reflection albedos vary in order to fit the light curves, and the results are albedos greater than those theoretically predicted for such stars. The  $\beta$  exponents assumed in these works are smaller than they should be according even to our non-grey results, possibly yielding an incorrect determination of the higher reflection albedos.

As stressed both in Paper I and by Claret (1998), comparisons between the theoretical calculations and the empirical determinations of  $\beta$  available at present are problematic and inconclusive, although promising (see Fig. 3 of Paper I and Fig. 7 of Claret 1998). A possible test of the results presented here is to fit the light curves of Algol-type stars using our predicted  $\beta$  values, to see if it is possible to improve upon earlier results. Such tests are currently underway, with our results (of this work and Paper I, for  $\beta$ , and of Alencar & Vaz 1999, for the limb-darkening coefficients) being implemented in a version of the WD model for light curve synthesis and solution of eclipsing systems (Wil-

son & Devinney 1971, Wilson 1979, Vaz et al. 1995, Casey et al. 1998).

#### 4. Summary and conclusions

The most general result of the present paper is that we have demonstrated for the first time the influence of external illumination on the gravity–brightening exponent, showing that external illumination increases the value of  $\beta$ . This suggests that the classical value of  $\beta = 0.32$  may be too small for binary systems with close components.

The results presented here extend our results from Paper I for illuminated convective atmospheres, providing  $\beta$  in the range  $3\,700\text{ K} < T_{\text{eff}} < 7\,000\text{ K}$ , for varying amounts of external illumination and angles of incidence. For illuminated convective grey atmospheres the gravity–brightening exponent may be calculated from the effective temperature of the illuminated star, the external radiation angle of incidence, and the incident flux of radiation that reaches the continuum forming layers in the illuminated star. The general trend of  $\beta$  having a maximum in the  $T_{\text{eff}}$  range covered in this work is interpreted as being caused by an interplay between the convection and opacity properties of the atmosphere model.

For illuminated non–grey atmospheres the gravity–brightening exponent also depends on the spectral distribution of the incident flux. When  $T_{\text{h}}$  does not differ by more than  $\sim 25\%$  from  $T_{\text{eff}}$ , the results obtained with illuminated grey atmospheres may be used. For larger relative temperature differences, one needs to correct the relative incident flux with a penetration factor, corresponding to the absorption of UV flux in the upper layers of the illuminated model. The penetration factor is necessarily a function of the metal abundance of the atmosphere, but this aspect has not been studied in the present paper.

*Acknowledgements.* SHPA and LPRV were supported in part by FAPEMIG, CNPq, FINEP, CAPES (Brazilian institutions). ÅN was supported in part by the Danish National Research Foundation, through its establishment of the Theoretical Astrophysics Center. Fruitful discussions with Drs. B.E. Helt and J.V. Clausen are gratefully acknowledged. The comments of an anonymous referee were fundamental to bring this work to its final form.

#### References

- Alencar S.H.P., Vaz L.P.R., 1997, *A&A* 326, 257 (Paper I)  
 Alencar S.H.P., Vaz L.P.R., 1999, *A&AS* 135, 555  
 Bell R.A., Eriksson K., Gustafsson B., Nordlund Å., 1976, *A&AS* 23, 37  
 Casey B.W., Mathieu R.D., Vaz L.P.R., Andersen J., Suntzeff N.B., 1998, *AJ* 115, 1617  
 Claret A., 1995, *A&AS* 109, 441  
 Claret A., 1998, *A&AS* 131, 395  
 Gustafsson B., Bell R.A., Eriksson K., Nordlund Å., 1975 *A&A* 42, 407  
 Khallesseh B., Hill G., 1992, *A&A* 257, 199  
 Kippenhahn R., Weigert A., Hoffmeister E., 1967, in *Computational Physics*. Academic Press, New York, Vol. 7, p. 129  
 Kurucz, R.L., 1979, *ApJS* 40, 1  
 Lucy L.B., 1967, *Zeitschr. für Astrophys.* 65, 89  
 Maxted P.F.L., Hill G., Hilditch R.W., 1994, *A&A* 285, 535  
 Maxted P.F.L., Hill G., Hilditch R.W., 1995, *A&A* 301, 141  
 Mihalas D., 1978, in *Stellar Atmospheres*, W.H. Freeman and Co., Chapter 3  
 Nordlund Å., Vaz L.P.R., 1990, *A&A* 228, 231  
 Vaz L.P.R., Andersen J., Rabello Soares M.C.A., 1995, *A&A* 301, 693  
 Vaz L.P.R., Nordlund Å., 1985, *A&A* 147, 281  
 von Zeipel H., 1924, *MNRAS* 84, 665  
 Wilson R.E., 1979, *ApJ* 234, 1054  
 Wilson R.E., Devinney E.J., 1971, *ApJ* 182, 539